PULSE PERFORMANCE ANALYSIS FOR SMALL HYPERGOLIC-PROPELLANT ROCKET ENGINES

Gerald W. Smith

and

Richard H. Sforzini

April 13, 1972

Backup Document for AIAA Synoptic Scheduled

for Publication in the Journal of Spacecraft and Rockets

August 1972

George C. Marshall Space Flight Center

National Aeronautics and Space Administration

Huntsville, AL 35812

SYNOPTIC BACKUP DOCUMENT

This document is made publicly available through the NASA scientific and technical information system as a service to readers of the corresponding "Synoptic" which is scheduled for publication in the following (checked) technical journal of the American Institute of Aeronautics and Astronautics.

- ☐ AIAA Journal
- ☐ Journal of Aircraft
- ☒ Journal of Spacecraft & Rockets, August, 1972
- ☐ Journal of Hydronautics

A Synoptic is a brief journal article that presents the key results of an investigation in text, tabular, and graphical form. It is neither a long abstract nor a condensation of a full length paper, but is written by the authors with the specific purpose of presenting essential information in an easily assimilated manner. It is editorially and technically reviewed for publication just as is any manuscript submission. The author must, however, also submit a full backup paper to aid the editors and reviewers in their evaluation of the synoptic. The backup paper, which may be an original manuscript or a research report, is not required to conform to AIAA manuscript rules.

For the benefit of readers of the Synoptic who may wish to refer to this backup document, it is made available in this microfiche (or facsimile) form without editorial or makeup changes.

PULSE PERFORMANCE ANALYSIS FOR SMALL HYPERGOLIC-PROPELLANT ROCKET ENGINES

Gerald W. Smith*
NASA Marshall Space Flight Center, Huntsville, Ala
and
Richard H. Sforzini**
Auburn University, Auburn, Ala.

Abstract

Small rocket engine tests were conducted for the purpose of obtaining pulse performance data to aid in preliminary design and evaluation of attitude control systems. Both monopropellant and hypergolic bipropellant engines of thrust levels from 1 to 100 lbs. were tested. The performance data for the hypergolic propellant rockets are compared with theoretical performance calculated from idealized chamber filling and evacuation characteristics. Electromechanical delays in valve response and heat transfer characteristics were found to cause substantial deviation between theoretical and test performance.

All data were obtained from rocket tests conducted at the NASA Marshall Space Flight Center, Huntsville, Alabama. Analysis of data and development of the pulse prediction model were accomplished at Auburn University in conjunction with the Master of Science in Aerospace Engineering program of Gerald W. Smith.

* Aerospace Engineer, Power and Propulsion Branch, Astronautics Laboratory, Associate Member AIAA.

** Professor, Aerospace Engineering, Associate Fellow AIAA.

The theoretical analysis is modified to obtain a semi-empirical model for hypergolic propellant rockets which is demonstrated to be reasonably accurate for two different engine configurations over a considerable range of duty cycles.

Nomenclature

A	=	cross-sectional area
c_f	=	engine thrust coefficient
c_p, c_v	=	specific heat at constant pressure and constant volume, respectively
c^*	=	characteristic exhaust velocity $\equiv \sqrt{RT_c} / \Gamma$
F	=	engine thrust
I_{sp}	=	specific impulse
I_t	=	total impulse
L^*	=	engine characteristic length $\equiv V_c/A_t$
M	=	Mach number
m	=	mass
P	=	pressure
R	=	universal gas constant
t	=	time
V	=	volume
u	=	velocity relative to vehicle
γ	=	ratio of specific heats $\equiv c_p/c_v$
Γ	=	$(\gamma)^{1/2} [2/(\gamma+1)] (\gamma+1)/2(\gamma-1)$
$(\bar{})$	=	average value
$(\dot{})$	=	differentiation with respect to time

Subscripts

a	=	atmospheric condition
c	=	chamber condition
d	=	discharge condition
f,o	=	fuel and oxidizer injected, respectively
p	=	propellant (fuel plus oxidizer) injected
e,t	=	nozzle exit and throat, respectively
s	=	steady state condition

Introduction

The direction of the nation's space exploration program toward missions with longer lifetimes, such as the Apollo, Skylab, and Mars missions, has created new design and stringent operational requirements for launch vehicles and spacecraft subsystems. The attitude control system (ACS) provides rocket impulse for vehicle orientation and orbital or plane maneuvers. In the past, mission requirements for ACS have been primarily suborbital or satellite oriented, requiring relatively low thrust levels and total impulse (I_t). A typical satellite mission would require total impulses of less than 10,000 lbf-sec with a resulting subsystem weight of a few hundred pounds. For systems of this size, reliability, simplicity, and use of state-of-the-art technology tend to be the major design criteria; performance is of secondary consideration. However, as mission lifetime and required total impulse and system weight increase, more emphasis must be placed on performance as a major design criterion. From the requirement for improved performance, two basic system designs have emerged, one a monopropellant, and the other bipropellant.

The monopropellant system utilizes a single propellant, anhydrous hydrazine (N_2H_4) and a catalyst bed which decomposes the propellant. The temperature of decomposition ranges from 1600° to 1800°F with a theoretical vacuum specific impulse (I_{sp}) of approximately 260 seconds. The bipropellant system (Fig. 1) uses two propellants, an oxidizer and a fuel, which are hypergolic. The most commonly used oxidizer is nitrogen tetroxide (N_2O_4), a liquid which is hypergolic with many fuels. Most common among the fuels are the various derivatives of hydrazine, a toxic liquid which is very flammable and ignites spontaneously in contact with N_2O_4. In contrast to the rather low chamber temperature of the monopropellants, the flame temperature of these bipropellants may be as high as 5500°F with a theoretical vacuum specific impulse of approximately 330 seconds.

The sizing of an attitude control system requires that the engine performance be known for the entire mission duty cycle. Test results have shown that the specific impulse (I_{sp}) varies with the engine duty cycle (Fig. 2). Determining with any degree of accuracy the impulse performance versus duty cycle for a given engine configuration is not a straightforward task and usually requires a test program designed to simulate the mission duty cycle and the engine operating environment. The capability of predicting the engine performance for specific operating conditions within reasonable accuracy limits would therefore be a very useful tool for the system designer.

The analytical determination of the thrust - time curve can be divided into four parts: (1) the pressure history up to the point of ignition, (2) the pressure history during the ignition process, (3) steady-state operation, and (4) the pressure during tailoff. For the case of very short pulses, the thrust

trace may be completely transient. An accurate performance model must include all portions of the trace from valve signal initiation through pressure decay. The reaction mechanism and the combustion characteristics of the propellants dictate the pressure and temperature environment within the combustion chamber. The major portion of this investigation and the test data which are used as a basis for the performance model are based on a nitrogen tetroxide (N_2O_4) monomethylhydrazine (MMH) hypergolic propellant combination whose general characteristics are given in Ref. 1.

Analytical prediction models exist which predict with reasonable accuracy the performance that can be expected with a fairly comprehensive selection of propellant combinations if the propellant atomization characteristics are known. Several theoretical studies have been made to describe the combustion of liquid sprays under the assumption that propellant vaporization is the rate controlling process.[2] The droplet size and distribution must be known in order to predict the engine performance. Accurate measurements of the degree of atomization and propellant mixing in an actual rocket engine environment are extremely difficult to achieve, although attempts at such measurements have been made with high speed photography, laboratory or scale model tests, and various gas sampling techniques. Detailed discussion of the interrelations among injector design, atomization, vaporization and combustion efficiency are given by Lewis, Ingebo, Miesse, Priem, and Penner.[2-7] Analysis of performance of hypergolic propellants is further complicated because reaction may occur in both liquid and gaseous states. Tests indicate that below certain critical pressure and temperature limits the initial reaction occurs in the liquid phases, whereas for higher pressures and temperatures, normal gas-gas reaction occurs.[8, 9] Release of the propellants into a confined region such as a combustion chamber under space

vacuum conditions results in a rapid pressure rise just due to vaporization of the oxidizer. This results in primarily a gaseous phase reaction producing consistent and repeatable start transient characteristics even at very low ambient pressure conditions.

Clearly ignition delay time and the start transient after ignition are very important factors in determining the impulse developed by an engine during a short pulse. The ignition delay time has been somewhat arbitrarily defined as that time interval required to generate a sufficient quantity of intermediates in the rate controlling reaction step so that product gases near the adiabatic flame temperature are produced.[10] For N_2H_4 - N_2O_4 propellant combination the rate controlling step is highly exothermic so that the product gases are those generated during this reaction. Because of the high temperatures, subsequent reactions occur very quickly. The suggested kinetics for the reaction is [10]:

$$2N_2H_4 + N_2O_4 \longrightarrow 3N_2 + 4H_2O \qquad (1)$$

although there is some evidence that the mechanism of the reaction involves an initial neutralization followed by an oxidation, or

$$N_2H_4 + N_2O_4 \longrightarrow 2N_2 + 2H_2O + O_2 \qquad (2)$$

$$O_2 + N_2H_4 \longrightarrow N_2 + 2H_2O \qquad (3)$$

Experimental measurements of ignition delay times using hydrazine-nitric acid mixtures yield results from 0.1 to 3 milliseconds and flame speeds of approximately 200 ft/sec are indicated.[11] For small rocket motors, 3 inches in length or diameter, the length of time required for a flame to sweep the chamber is about 1 millisecond. Once ignition is achieved, the chamber pressure transient depends on the amount of propellant inside the chamber. A model for predicting

hypergolic ignition transients in space engines is presented by Seamans.[12] This analysis treats the pressurization of a thrust chamber as a sequence of steady-state processes in very short time intervals considering the effects of vaporization and the chemical kinetics of the propellant reaction. The model does not account for varying injector flow rates which occur during the start transient as a result of flashing of such highly volatile propellants as N_2O_4, which appears to play an important role in the actual start characteristics.

After the start transient is completed, the engine achieves a steady-state operating condition. The chamber pressure and temperature during this phase of operation remain approximately constant as governed by flow rates, mixture ratio, and geometric factors. The fourth and final portion of the pulse that must be modeled is the pressure decay or tailoff. Most analytical models describe the shutdown sequence as an instantaneous stopping of the burned gas generation followed by an immediate decay in chamber pressure. Two examples of these models assume isentropic and isothermal decay rates inside the combustion chamber.[13, 14] As is shown later in the article, these idealizations again fail to give an accurate representation of the transient behavior. Furthermore, the pressure response of the engine during both start-up and shut-down does not occur instantaneously upon electrical command to the engine valves. Examination of rocket engine flow data reveals lags in the flow rate response. All of these factors will tend to reduce the accuracy of any theoretical type performance prediction model such that, for short pulses of less than 100 msec duration, theoretical results may be grossly inaccurate. This article explores these areas to a somewhat greater extent in order to determine their significance and to establish a more accurate prediction model based on empirically derived information.

Experimental Investigation

Both monopropellant and hypergolic bipropellant engines of separate thrust levels (1 to 100 lb.) were tested. Although various engine configurations were tested, the test data presented and those data that were used as the basis for the empirical model were obtained from tests of bipropellant engines using N_2O_4-MMH propellants. The basic features of the test engines are summarized in Table 1.

Table 1. Description of test engines

Test configuration	Engine A	Engine B
Propellants	N_2O_4/MMH	N_2O_4/MMH
Thrust, lbf(vacuum)	100	22
Chamber pressure, psia	142	95
Mixture ratio, O/F	1.6	1.6
Nozzle expansion ratio, A_e/A_t	60:1	40:1
Throat area, $in.^2$	0.397	0.1327
Injector configuration	Multiple element unlike impinging doublet	Single element impinging doublet
Characteristic length, L*, in.	11.0	7.0
Cooling technique	Film & radiation	Radiation
Boundary layer coolant, $\%\dot{m}_f$	40.0	0

Engine A was selected as the primary data source based on engine configuration, quality of the test data, and the type of instrumentation used during the test. Tests on engine B were not conducted for the specific purpose of analysis of

pulse performance, but sufficient information was obtained to provide a reasonable basis of comparison with engine A. In certain instances, test data from a second engine (B-1) identical to B are included for additional analysis purposes. Engines A and B are considered to be very representative of current state of the art for attitude control engines both in terms of hardware design and performance.

The propellant valve for engine A was torque motor operated with mechanically linked oxidizer and fuel valves. The valve poppets were held in the closed position by permanent magnet biasing forces on the torque motor. Two welded flexure tubes provided redundant seals to prevent the propellants from intermixing and to isolate the torque motor from the propellant. The design was of all-welded, corrosion-resistant steel construction with a "soft" seat teflon seal at each nozzle orifice to minimize leakage. Solenoid valves were used for propellant control for engine B.

A steam ejector system with diffuser was used to maintain near vacuum conditions in the vacuum test chamber. The ejector system was capable of simulating an altitude of 82,000 feet at propellant flow rates of 0.40 lb/sec (approximately 100 lbf thrust) and 115,000 feet at 0.10 lb/sec (approximately 25 lbf). When the engine was not firing, the pressure inside the vacuum chamber was maintained at 0.059 psia, or 125,000 feet. The vacuum chamber was approximately 3 feet in diameter and 3 feet long. The engines were mounted horizontally on a thrust measuring test bed which utilized a Flexcell consisting of a load cell and a parallelogram flexure. The primary instrumentation used for the performance analysis were propellant flow rates and temperatures, engine chamber pressure, and valve current. Redundant (series mounted) flowmeters were used in each propellant line in order to obtain accurate flow measurements. Both a turbine type flowmeter and a Ramapo flow transducer were used.

Pre-test and post-test calibrations indicated that the Ramapo transducer was the more accurate of the two and was also found to be more responsive to pulse flow measurements than the turbine type, which had greater inertia to overcome during flow transients. The turbine flowmeter was primarily used to validate steady-state readings. The Ramapo flow transducer senses the dynamic force of fluid flow as a drag force on a specially contoured body of revolution suspended in the flow stream. This force is transmitted by a lever rod and modified coaxial torque tube to an externally bonded, four-active-arm strain gage bridge. The absence of bearings, linkages, and moving parts provides high-frequency response with inherently low hysteresis.

The combustion chamber pressure was measured by a close coupled strain gage pressure transducer capable of a rise time of 1.0 millisecond or less from 10 to 90 percent of any pressure step input with an overshoot of less than 10 percent of the pressure step. For most test runs the transducer was mounted approximately 6 inches from the chamber and connected by 1/8-inch tubing to the chamber wall. This resulted in a fill volume of 0.0588 $in.^3$, which produced negligible effect on pressure response time. Immersion type thermocouples and pressure transducers were used to measure propellant conditions just upstream of the engine valves. Thermocouples on the chamber and nozzle walls were used to determine external skin temperatures.

All data signals were recorded on strip chart recorders with propellant feed pressure, chamber pressure, valve current, and flow rates also being recorded on oscillograph recorders and analog magnetic tape. Steady-state specific impulse and characteristic exhaust velocity were calculated from strip chart recorder data obtained during the steady state portions of the test run.

This proved to be the most accurate method for calculating steady-state performance. Pulse performance calculations were based on the oscillograph and analog tape data.

The same test duty cycle was used for each engine in order to provide a common base for performance comparison and to characterize the engine performance over a range of operating conditions. The duty cycle (table 2) was considered representative of ACS missions under consideration at the time the test program was conducted.

Typical test results as recorded by oscillograph are shown in Fig. 3. The thrust trace was very erratic throughout the test and therefore values of thrust calculated from the chamber pressure were substituted for performance analysis. The difficulty was attributed to overheating of the strain gages attached to the Flex-cell. The transient response characteristics of other engines are illustrated in Fig. 4. The data presented were obtained from tests which for the most part were not instrumented for pulse performance analysis. The slow rise and decay in propellant flow rates is indicative of the data obtained from a turbine-type flowmeter with a slow response. The oscillograph traces show the erratic nature of the flow transients during pulsing operation. Such behavior is caused by pressure pulses in the engine feed lines produced by rapid opening and closing of engine valves and is influenced by feed line size, volume between valve and injector, and propellant temperature. These unstable flows make it extremely difficult to either model or to accurately measure pulse performance of the engine.

For operation at high altitudes or in near vacuum conditions, once choked flow is achieved in the nozzle the thrust coefficient c_f remains essentially

Table 2. Engine test duty cycle[a]

Step	Number of Cycles	On-time (sec)	Off-time (sec)
1	10	0.03	100.0
2	10	0.10	100.0
3	10	0.30	100.0
4	10	3.0	100.0
5	10	0.03	10.0
6	10	0.10	10.0
7	10	0.30	10.0
8	10	3.0	10.0
9	20	0.03	1.0
10	20	0.10	1.0
11	20	0.30	1.0
12	20	3.0	1.0
13	20	0.03	0.10
14	20	0.10	0.10
15	20	0.30	0.10
16	20	3.0	0.10
17	5-minute steady state run		

a. Total engine on-time = 505.8 seconds

constant. For very low ambient pressure conditions the flow will be choked almost instantaneously with the first measurable amount of chamber pressure. The thrust, then, depends only on chamber pressure variation with time, and engine specific impulse for a single pulse can be determined from

$$I_{sp} = A_t c_f \int P_c dt \,/ \int \dot{m}_p dt \qquad (4)$$

Specific impulse for each step (Table 2) was calculated from the recorded data using equation 4. The results for engine A are those given in Fig. 2. The values plotted are the averages for two pulses only as the pulse-to-pulse variations are quite small.

Data Analysis

The feasibility of adopting a semi-empirical approach was investigated by analyzing the test data obtained from engine A. The pressure and flow transients (buildup and decay) appeared to be quite repetitive regardless of duty cycle. The assumption was therefore made that propellant flow rates and chamber pressure are relatively insensitive to duty cycle condition and depend mainly on a pulse time reference. This assumption is not valid for cases where the time between pulses is of such a short duration that the chamber pressure and flow rates have not had time to completely decay prior to the next pulse. In these instances, allowances must be made for the non-zero start conditions in addition to the possibility of differences in the start transient behavior. This is best illustrated in Fig. 5, where the oxidizer flow transient is entirely different from that of other pulses presented in Figs. 3 and 4. The present analysis is restricted to duty cycles where the off-time is sufficient to allow the pressure and flow rates to decay completely.

Figures 6 and 7 show more clearly the variation of pressure with pulse on-time for A and B respectively. A delay of the order of 10 msec. is noted before any pressure rise occurs. These delays are attributed to the electromechanical characteristics of the valve, the hydraulic response characteristics of the propellants, and the ignition initiation delay. Similar lags are notable at cutoff and affect mass flow rate responses as well as the pressure changes. The largest portion of the lags may be traced to the valve response which has been measured at 6 msec. for opening and closing respectively. For the purpose of this analysis, it is assumed that the rise and decay lags are known or can be reasonably estimated.

As a first approach toward establishing a mathematical model of the start transient, it is further assumed that the propellant burns at a constant rate equal to the steady state propellant injection rate. The continuity equation establishes a balance between the mass flow rate of propellant $\dot{m}_p$, the mass discharge rate through the nozzle $\dot{m}_d$ and the rate of change of gaseous mass within the combustion chamber:

$$\dot{m}_p = \dot{m}_d + d(\rho_c V_c)/dt \tag{5}$$

For small engines, it may be assumed that $\dot{m}_d$ is given by the steady state nozzle discharge equation:[14]

$$\dot{m}_d = P_c A_t / c^* \tag{6}$$

It is next assumed that the gases are perfect ($\rho_c = P_c/RT_c$) and that T_c is constant during pressurization. Equations (5) and (6) then yield

$$dt = dP_c/[c^*\Gamma^2 (\dot{m}_p c^* - P_c A_t)/V_c] \tag{7}$$

which when integrated gives

$$P_c = P_{cs}\left[1 - e^{(c^*\Gamma^2/L^*)t}\right] \tag{8}$$

The result is superimposed on the plot of the test data in Figs. 6 and 7. Although substantial differences exist between the theoretical and actual performance, Equation 8 establishes a plausible basic form for the pressure transient.

The solid lines in Figures 6 and 7 are the results of fitting an equation of the basic form of Equation 8 to the test data and modifying the equation by the addition of a constant, "k", in the exponential term. A "k" value of .036 yields good correlation with the test data for both engines A and B. A deviation was found to exist between the empirically derived values and the experimental data during the latter part of the pressure rise transient for engine A (Figure 6). This was not true for engine B and would appear to be caused by differences in the thermal response characteristics of the two engines (discussed later).

Most theoretical models of the pressure decay transient describe the shutdown sequence as an instantaneous stopping of the gas generator followed by either isentropic or isothermal depressurization. For the isentropic case, the continuity equation gives for the time after cutoff[13]

$$t = (L^*/\Gamma^2 c^*)\,[2/(\gamma - 1)]\left[(P_{cs}/P_c)^{\frac{\gamma - 1}{\gamma}} - 1\right]^{1/2} \tag{9}$$

for the isothermal case, the result is

$$P_c = P_{cs}\left[e^{-(\Gamma^2 c^*/L^*)t}\right] \tag{10}$$

Both isentropic and isothermal rates of decay give numerical results showing a chamber pressure of 2 psi in less than 4 msec. The actual test results illustrated in Figs. 8 and 9 indicate substantially longer decay rates. The exponential form of the decay transient equation is adopted to describe the shutdown transient again using the constant k in the exponential term. Curve fitting of the test data again revealed that a k value of .036 best described the shutdown transient for both engines as noted by the solid lines in Figs. 8 and 9. Thus a large degree of similarity is seen to exist in both the form of the start and shutdown transient equations and also the k factor for both engines A and B. For engines B and B1 the decay transient appears to be independent of the duty cycle, whereas for engine A the longer pulse on times tend to produce longer decay transients (Fig. 8).

A possible explanation for the decrease in decay rates with an increase in pulse width is that the engine chamber wall temperature increases as the pulse duration increases. As the gas remaining inside the chamber starts to expand after the propellant flow ceases, the rate at which heat is transferred from the gas to the hot chamber wall is reduced thus causing the pressure decay to be slower than for the cooler wall cases. A lack of test data over a wide range of duty cycles would appear to explain why engine B did not exhibit a similar behavior during the decay transient.

As was true of the start transient, a lag time exists before the chamber pressure starts to decay. For engine A, this lag time is 6 msec. Since the pressure pulse is delayed 13 msec in the starting transient, and 6 msec in the decay transient, this means that for a 100 msec. electrical pulse width, an active pressure response (greater than 10% steady state pressure) will occur for a period of 93 msec. before the pressure decay is initiated.

In an attempt to better understand the differences in the transient behavior of engines A and B, the thermal histories of the engines during the start and shutdown transients were reviewed. Although only limited data was available for analysis, it was notable that engine B achieved thermal equilibrium in a fraction of the time required for engine A. There are several factors which could contribute to this: (1) engine A is film and radiation cooled, whereas B is only radiation cooled; (2) the dribble volume between the valve and injector are much larger for engine A than for B thus producing longer transients; (3) the larger chamber volume does not have a proportionally larger surface area which reduces the effect of heat transfer from the gas to the chamber wall. A detailed thermal analysis using additional instrumentation would be required in order to obtain a quantitative evaluation of the engine thermal characteristics.

To complete the mathematical model, expressions for the propellant flow rates must be obtained. The oxidizer flow start transient is shown in Figure 10, which illustrates the characteristic overshoot common to all engines of this type for both fuel and oxidizer. Several attempts were made to curve fit the transient by means of exponential expressions, but these failed to provide a reasonable degree of correlation with the test data. Furthermore, tailoring of equations to fit the unique characteristics of the propellant flow rates by use of a high degree polynominal results in a mathematical model applicable only to a specific engine configuration and is of little value in the performance prediction of other engines. Study of the test data indicated, however, that the assumption of a step flow rate at the steady

state level beginning with the first evidence of flow would provide a reasonable estimate of the gross response which is all that is needed for calculation of specific impulse. The flow lag for engine A was consistently 7 to 8 milliseconds after the valve open and close signal for both propellants and was found to be independent of duty cycle. Flow rate data for engine B are not included since high response flow transducers were not used with the engine.

Finally, the flow decay rates were analyzed and are presented in Figure 11. Straight-line approximations of the flow decay provided excellent correlation with the test data.

Results and Conclusions

Integration of the various equations for engine A gives the predicted performance shown by the solid line in Figure 2. A prediction based directly on idealized theoretical start and decay transients (Figs. 6 and 8) using experimental values for pressure and flow rate lag times is indicated by the dashed line on the figure. The use of theoretical expressions alone, without consideration for these lag times, would tend to shift the dashed line upward increasing the error between the predicted and experimental values for specific impulse. As expected, the empirical model agrees more closely with the test data throughout the entire duty cycle range. For pulse on times greater than 100 msec, the deviation between the model predicted value and the average test value at each pulse on time increment (Figure 2) is less than 10%. For the very short pulses, propellant overshoot characteristics in both the fuel and oxidizer, which are not accounted for in the model, become significant causing the model results to be somewhat higher than the actual test data. The higher performance for the shorter off-times with fixed pulse duration appear to be attributable to a combination of higher average pressure during the pulse and a reduced total propellant flow rate. It appears that the model could be

further refined by the use of another term to account for effects of off-time; however, without additional tests, the generality of the results could not be properly assessed.

The equations which describe the engine pressure and flow rate behavior were derived based on test data obtained from tests of 22 and 100 lbf engines representative of current auxiliary propulsion system engines. A large degree of similarity was found to exist in the equations describing the pulse transients and between the two engine configurations studied. This similarity in behavior indicates that an empirical model can be used to predict the performance of a varying range of engine sizes and configurations within reasonable accuracy limits.

The empirical model results were compared to several theoretical prediction techniques and were found to provide a much greater degree of correlation than the ideal equations. To adopt the empirical model without the benefit of additional test data, several characteristics of the engine should be established:

1. The valve opening and closing response times are required and can be determined by component tests. Usually, for ACS size engines, this time will vary between 3 and 8 milliseconds and will be constant for a given valve configuration. This factor determines the time lag for both the propellant flow rates and the pressure transients.
2. The size of the fill volume between the engine valve seat and the injector must be known, as it affects the length of time required for propellants to enter the chamber and thus influences the ignition lag time. The reaction time for the subject hypergolic propellants is so rapid that its effect on ignition delay is negligible.

3. The steady-state operating point can be determined using the characteristic exhaust velocity and the thrust coefficient (c_f) and efficiency factors based on past experience with similar designs. The propellant flow rates can be calculated with standard analytical procedures.
4. An assessment of the engine thermal characteristics should be made based upon analysis of the particular heat transfer situation or past test experience of the type described in the article.

The use of the above information in conjunction with the empirical model equations should result in performance prediction values which have a greater degree of accuracy than idealized theoretical prediction techniques and should provide accuracy levels within the ranges required for preliminary design.

The model described herein is based on limited test data. Data analysis of test results from engines of different sizes and configurations might tend to alter the model equations or even further validate the conclusions presented. In any event, a relatively simplified semi-empirical model has been demonstrated to be reasonably accurate for two very different engine configurations operating over a considerable range of pulse-on and pulse-off times.

References

[1]Duncan, A. F., Kelly, T. L., and Moberg, D. A., *A Study of Hypergolic Mass Expulsion for Attitude Control of Spacecraft,* The Marquardt Corporation, Technical Documentary Report No. AST-TR-62-1065, August 1964, pp. 545-551, 602-603.

[2]Lewis, J. D., *Combustion and Propulsion,* Fifth AGARD Colloquim, Braunschweig, April 6-13, 1962, pp. 144, 167.

[3]Ingebo, R. D., "Relation of Atomization and Rocket Combustion Performance," *Chemical Engineering Progress,* Vol. 58, No. 4, April 1962, pp. 74-76.

[4]Miesse, C. C., "On the Combustion of a Liquid Fuel Spray, *Sixth Symposium (International) on Combustion,* Yale University, New Haven, Connecticut, August 19-24, pp. 732-738.

[5]Priem, R. J., *Propellant Vaporization as a Criterion for Rocket-Engine Design; Calculations using Various Log-Probability Distributions of Heptane Droplets,* Lewis Flight Propulsion Laboratory, NACA TN 4098, October 1957.

[6]Priem, R. J., *Propellant Vaporization as a Criterion for Rocket-Engine Design; Calculations of Chamber Length to Vaporize Various Propellants,* Lewis Flight Propulsion Laboratory, NACA TN 3883, September 1958.

[7]Penner, S. S., *Chemical Rocket Propulsion and Combustion Research,* Gordon and Breach, New York, 1962, pp. 45-97.

[8]Wasko, R. A., "Reaction of Hydrazine and Nitrogen Tetroxide in a Low-Pressure Environment," *AIAA Journal,* Vol. 5, No. 1, August 1963, pp. 1919-1920.

[9]Simmons, J. A., Gift, R. D. and Spurlock, J. M., "Reactions and Expansion of Hypergolic Propellants in a Vacuum," *AIAA Journal,* Vol. 6, No. 5, May 1968, pp. 887-893.

[10]Agosta, V. D., and Kraus, G., "An Investigation of The Impulse Bit Developed by a Pulsed Liquid Propellant Rocket Engine," *Chemical Engineering Progress Symposium Series*, Vol. 60, No. 52, pp. 8-16, 1964, AIEC, New York.

[11]Kilpatrick, Baker, *A Study of Fast Reactions in Fuel-Oxidant Systems*, p. 196, Williams and Wilkens.

[12]Seamans, T. F., Vanpee, M., and Agosta, V. D., "Development of a Fundamental Model of Hypergolic Ignition in Space Ambient Engines," *AIAA Journal*, Vol. 5, No. 9, September 1967, pp. 1616-1624.

[13]Rodean, H. C., "Rocket Thrust Termination Transients," *ARS Journal*, Vol. 29, No. 6, June 1959, pp. 406-409.

[14]Barrère, M., Jaumotte, A., De Veubeke, B. F. and Vanderkerchove, J., *Rocket Propulsion*, Elsevier Publishing Company, 1960, pp. 244, 404, 622.

List of Illustrations

0
1
2
3
4
5
6

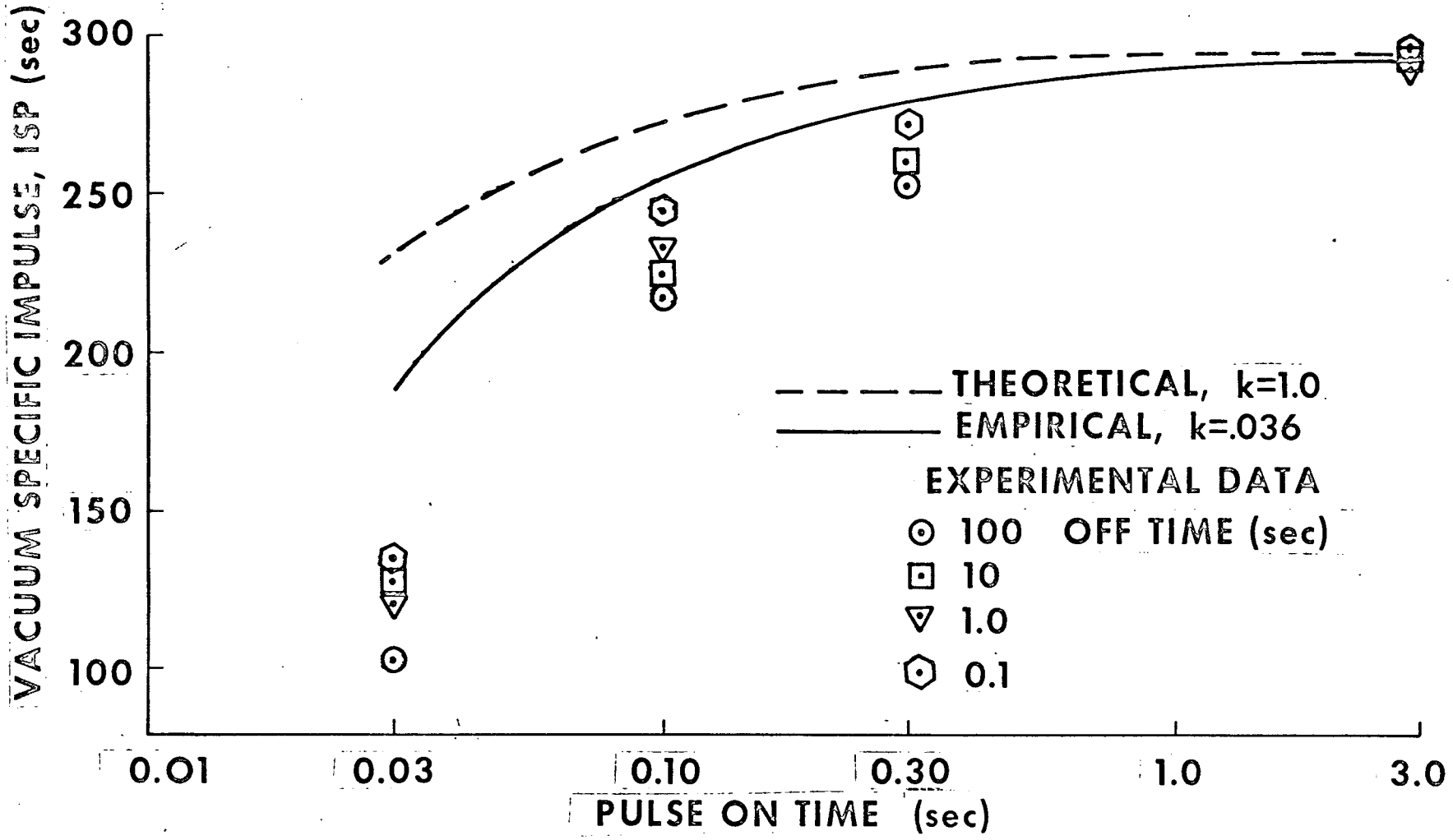
VACUUM SPECIFIC IMPULSE, ISP (sec)
300
250
200
150
100
0.01
0.03
0.10
0.30
1.0
3.0
PULSE ON TIME (sec)
THEORETICAL, k=1.0
EMPIRICAL, k=.036
EXPERIMENTAL DATA
100 OFF TIME (sec)
10
1.0
0.1

Fig. 2 [illegible]

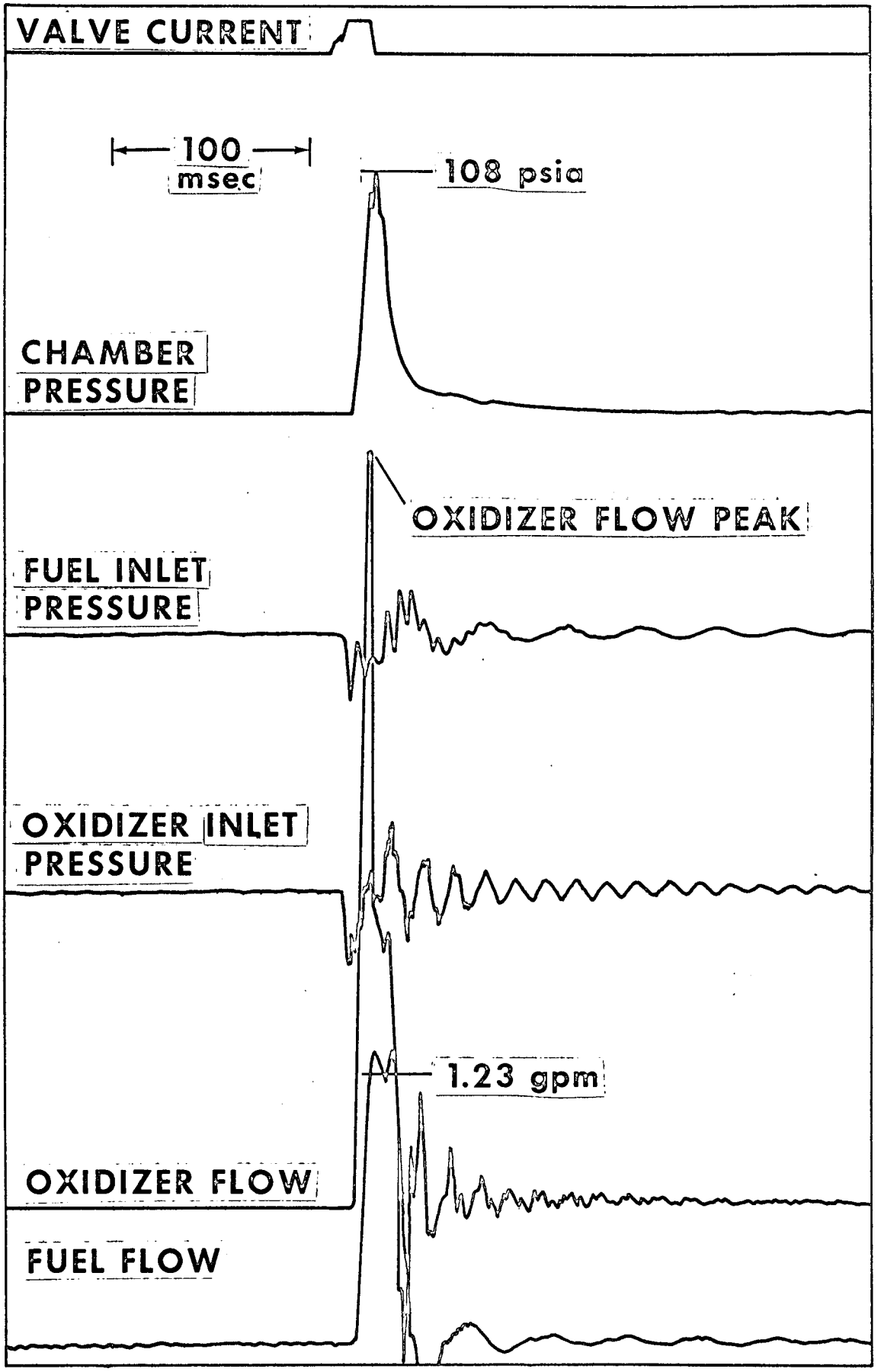
VALVE CURRENT
100
msec
108 psia
CHAMBER
PRESSURE
OXIDIZER FLOW PEAK
FUEL INLET
PRESSURE
OXIDIZER INLET
PRESSURE
1.23 gpm
OXIDIZER FLOW
FUEL FLOW

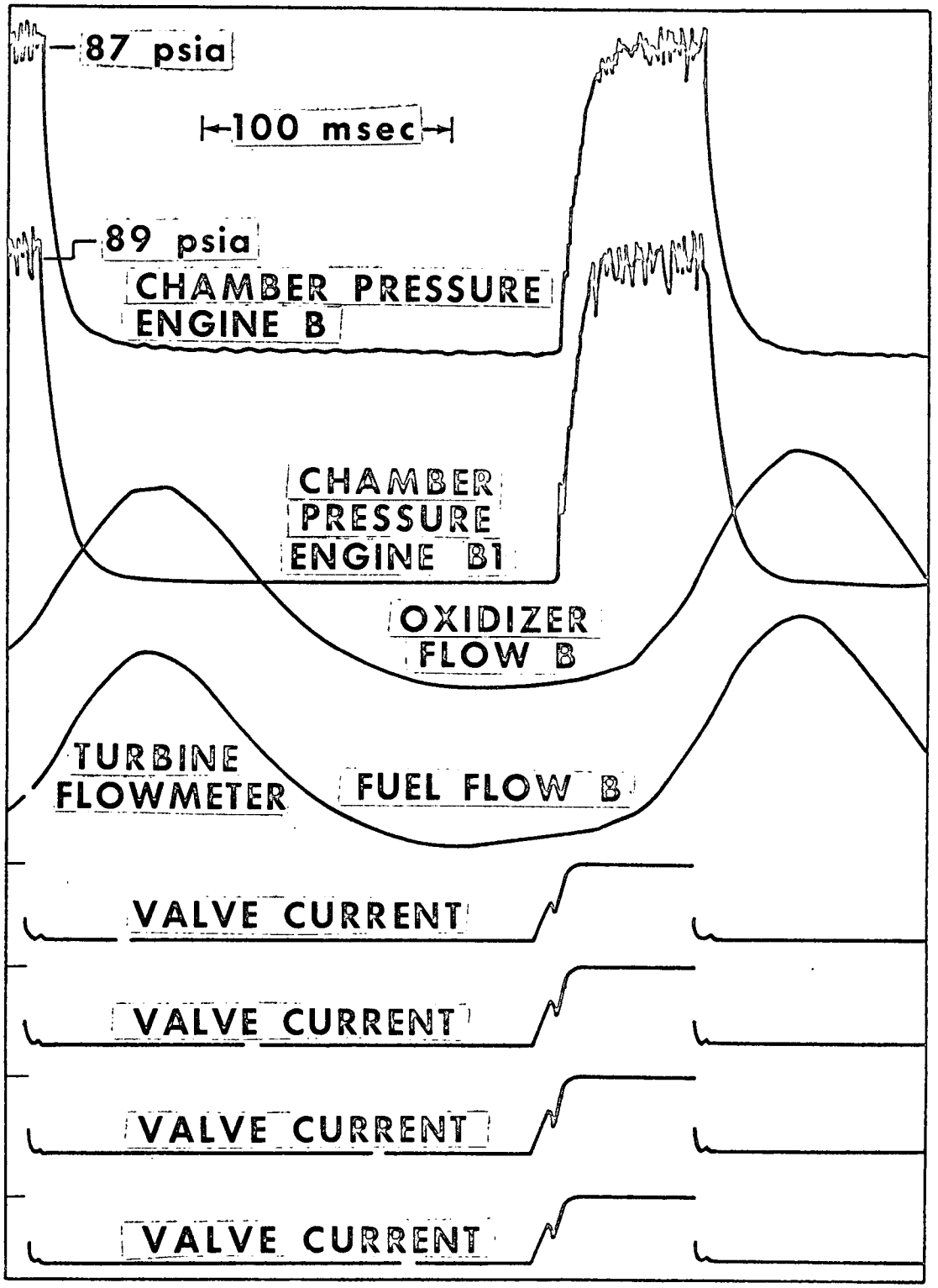
87 psia
100 msec
89 psia
CHAMBER PRESSURE
ENGINE B
CHAMBER
PRESSURE
ENGINE B1
OXIDIZER
FLOW B
TURBINE
FLOWMETER
FUEL FLOW B
VALVE CURRENT
VALVE CURRENT
VALVE CURRENT
VALVE CURRENT

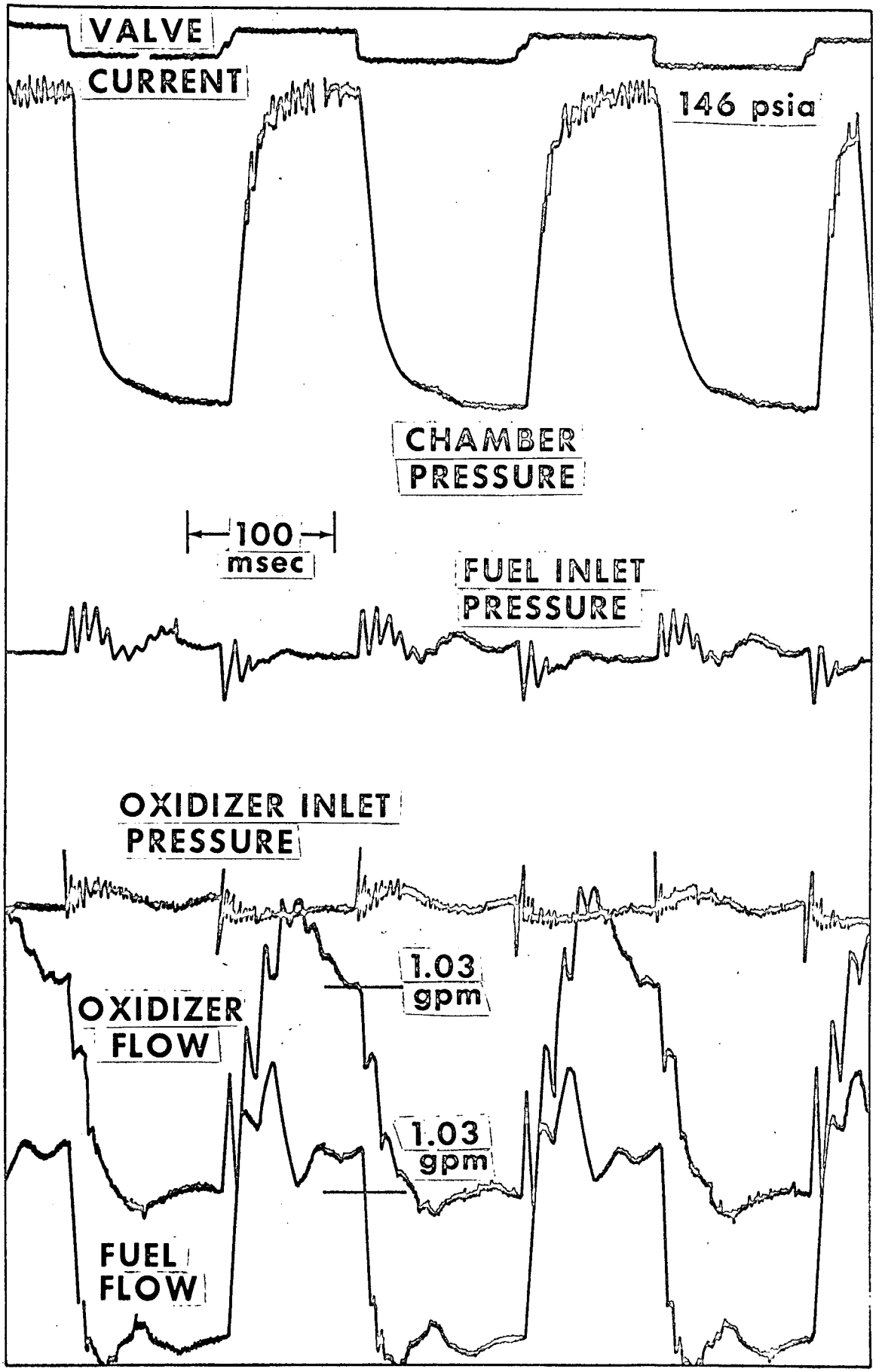
VALVE CURRENT
146 psia
CHAMBER PRESSURE
100 msec
FUEL INLET PRESSURE
OXIDIZER INLET PRESSURE
1.03 gpm
OXIDIZER FLOW
1.03 gpm
FUEL FLOW

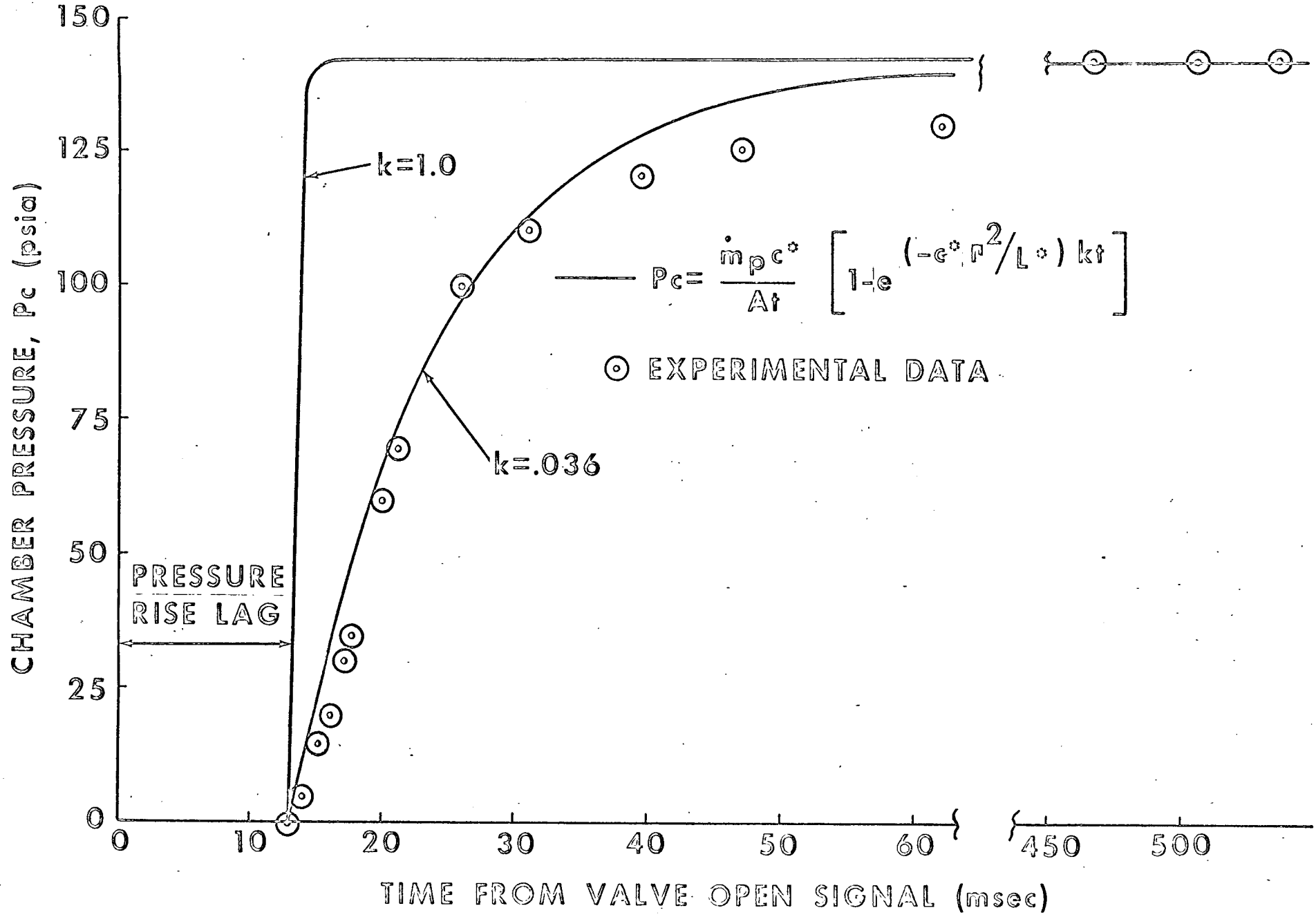
150
125
100
75
50
25
0
CHAMBER PRESSURE, Pc (psia)
k=1.0
k=.036
PRESSURE RISE LAG
$P_c = \frac{\dot{m}_p c^*}{A_t} \left[1 - e^{(-c^* \Gamma^2 / L^*) kt} \right]$
EXPERIMENTAL DATA
0
10
20
30
40
50
60
450
500
TIME FROM VALVE OPEN SIGNAL (msec)

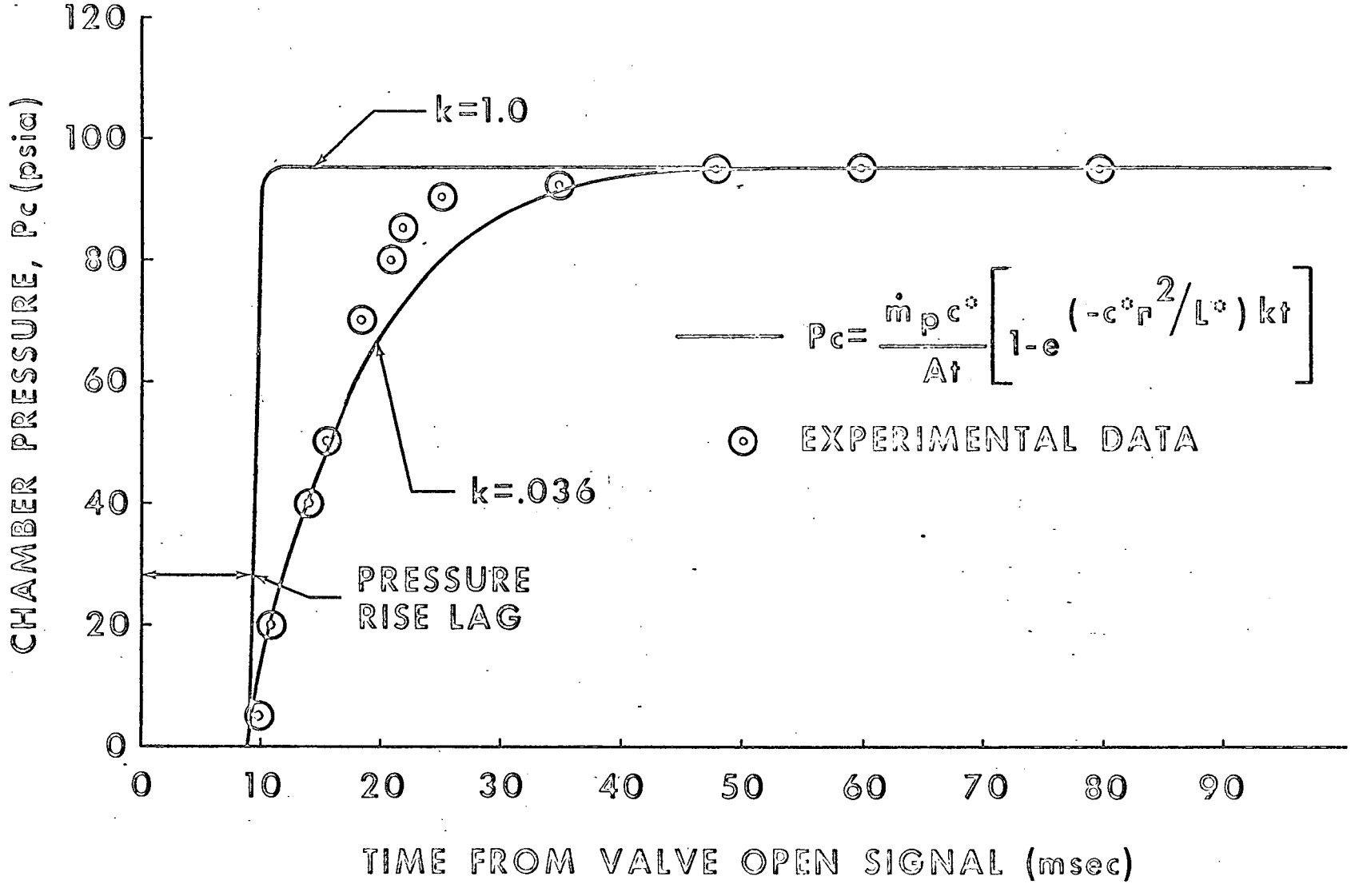
120
100
80
60
40
20
0
CHAMBER PRESSURE, Pc (psia)
k=1.0
k=.036
PRESSURE
RISE LAG
$P_c = \frac{\dot{m}_p c^*}{A_t}\left[1 - e^{(-c^* r^2/L^*)kt}\right]$
EXPERIMENTAL DATA
0
10
20
30
40
50
60
70
80
90
TIME FROM VALVE OPEN SIGNAL (msec)

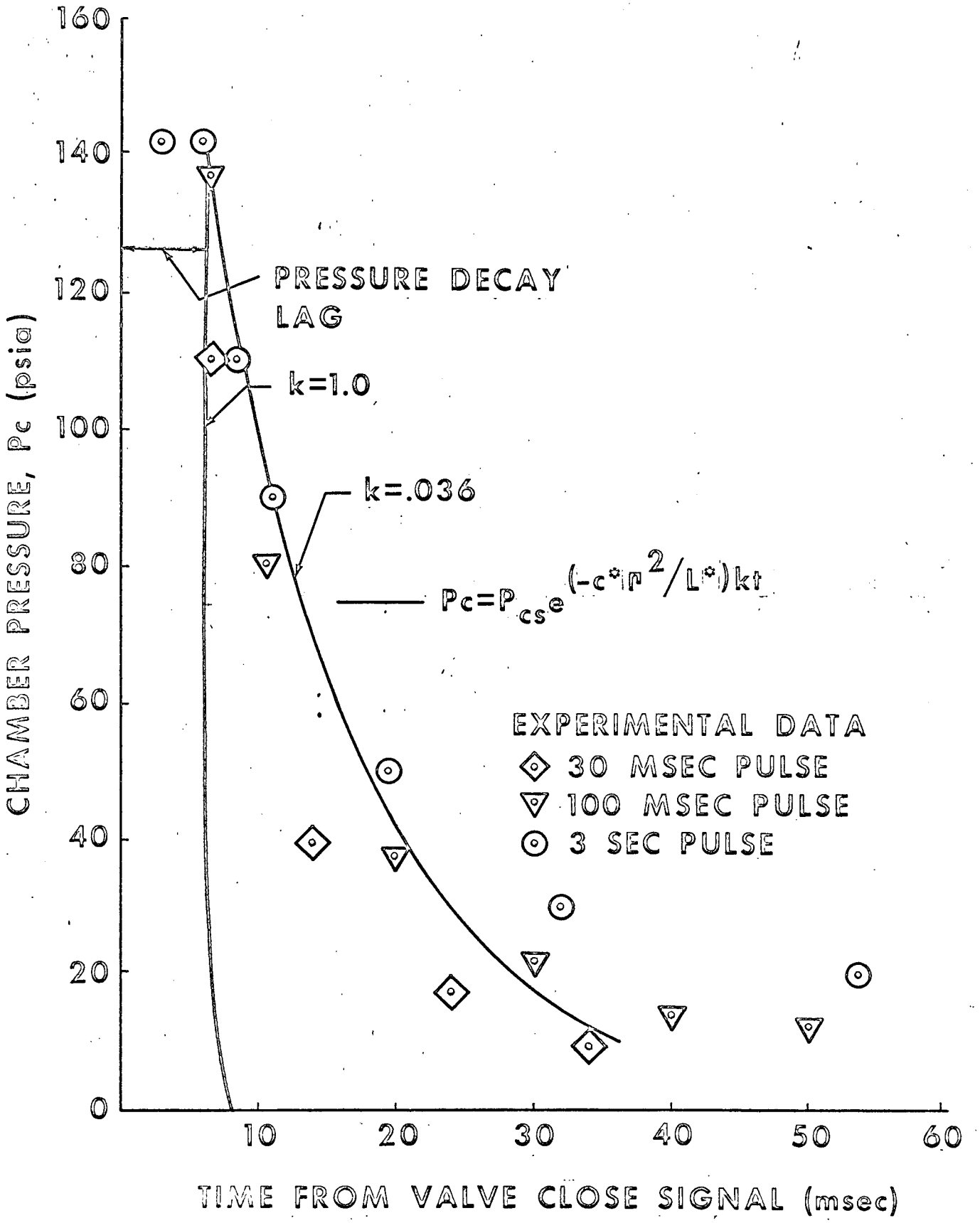
160
140
120
100
80
60
40
20
0
CHAMBER PRESSURE, Pc (psia)
PRESSURE DECAY LAG
k=1.0
k=.036
Pc=Pcs e(-c*r2/L*)kt
EXPERIMENTAL DATA
30 MSEC PULSE
100 MSEC PULSE
3 SEC PULSE
10
20
30
40
50
60
TIME FROM VALVE CLOSE SIGNAL (msec)

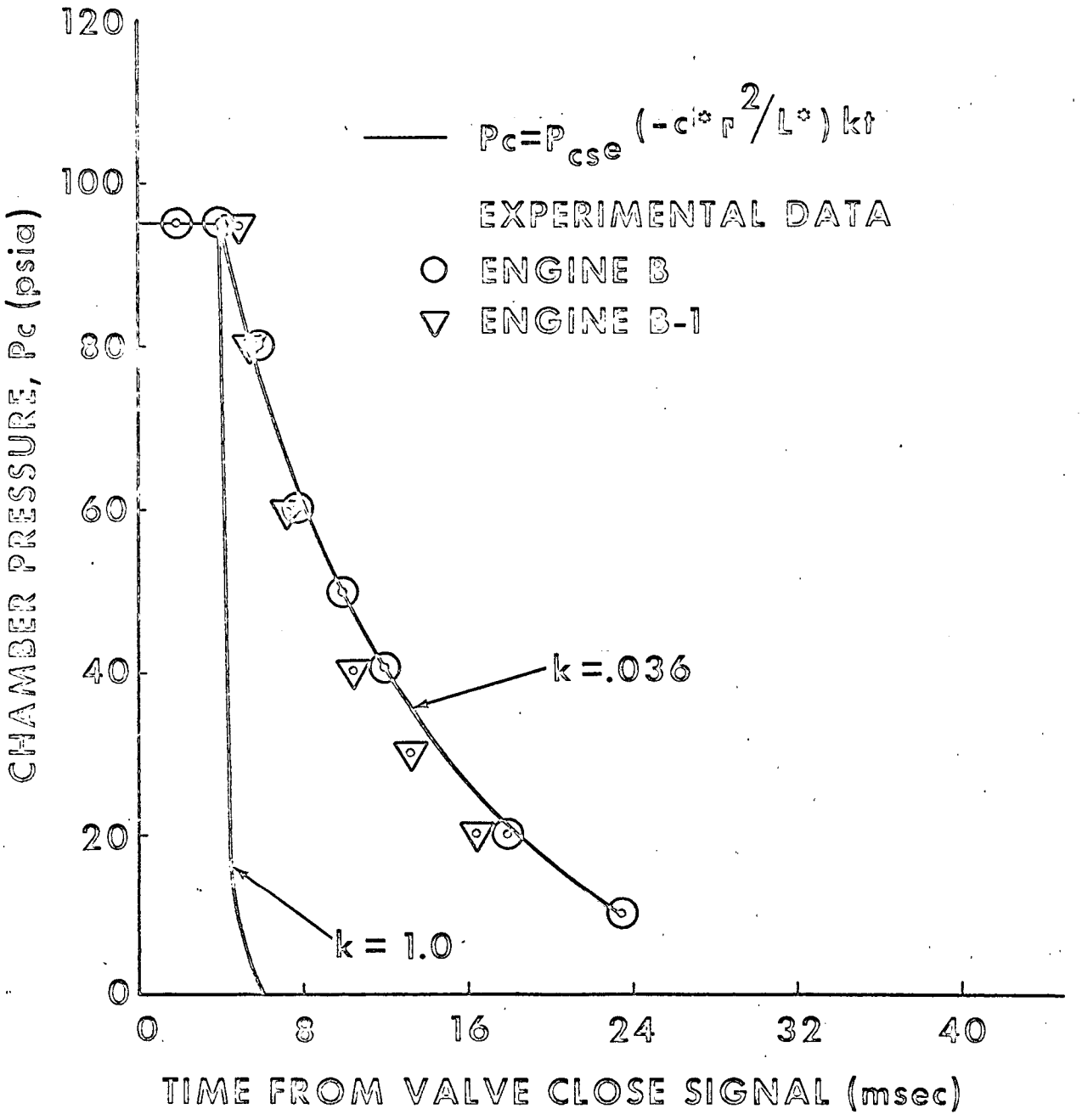
120
100
80
60
40
20
0
CHAMBER PRESSURE, Pc (psia)
$P_c = P_{cs} e^{(-c^* r^2/L^*) kt}$
EXPERIMENTAL DATA
ENGINE B
ENGINE B-1
k =.036
k = 1.0
0
8
16
24
32
40
TIME FROM VALVE CLOSE SIGNAL (msec)

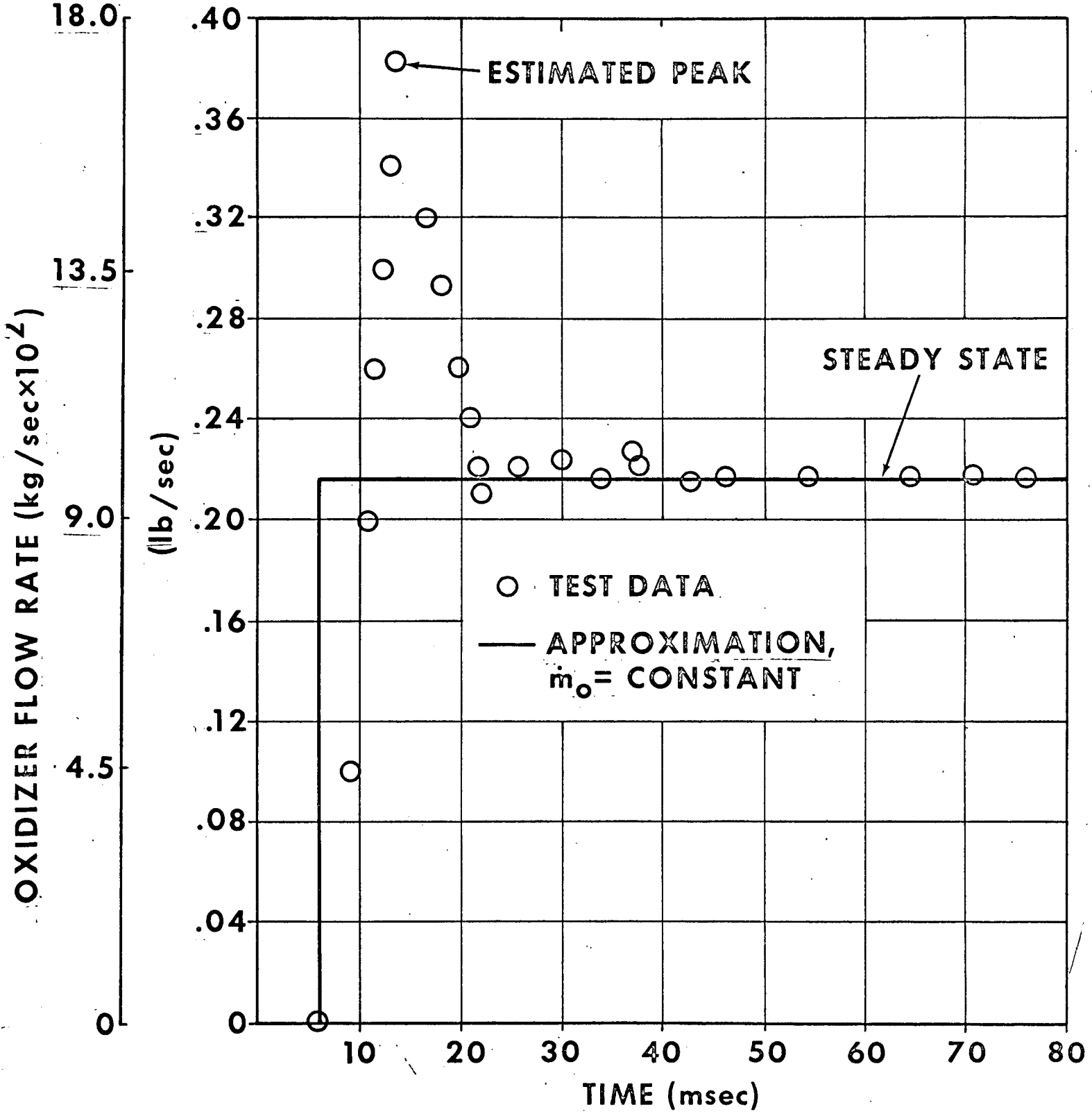
18.0
13.5
9.0
4.5
0
OXIDIZER FLOW RATE (kg/sec×10²)
.40
.36
.32
.28
.24
.20
.16
.12
.08
.04
0
(lb/sec)
ESTIMATED PEAK
STEADY STATE
TEST DATA
APPROXIMATION,
$\dot{m}_o$ = CONSTANT
10
20
30
40
50
60
70
80
TIME (msec)

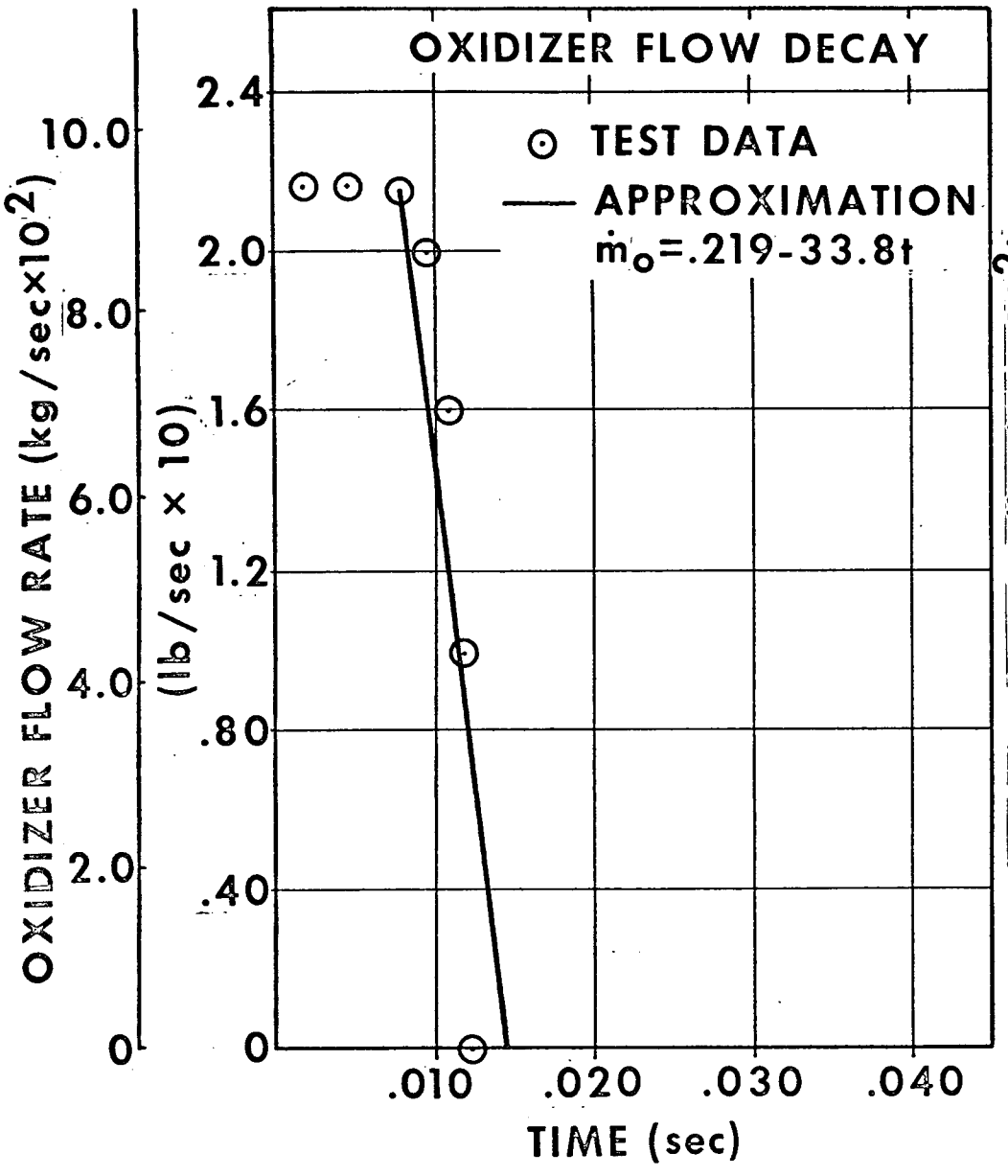
OXIDIZER FLOW DECAY
TEST DATA
APPROXIMATION
$\dot{m}_o$=.219-33.8t
OXIDIZER FLOW RATE (kg/sec×10²)
(lb/sec x 10)
TIME (sec)
10.0
8.0
6.0
4.0
2.0
0
2.4
2.0
1.6
1.2
.80
.40
0
.010
.020
.030
.040

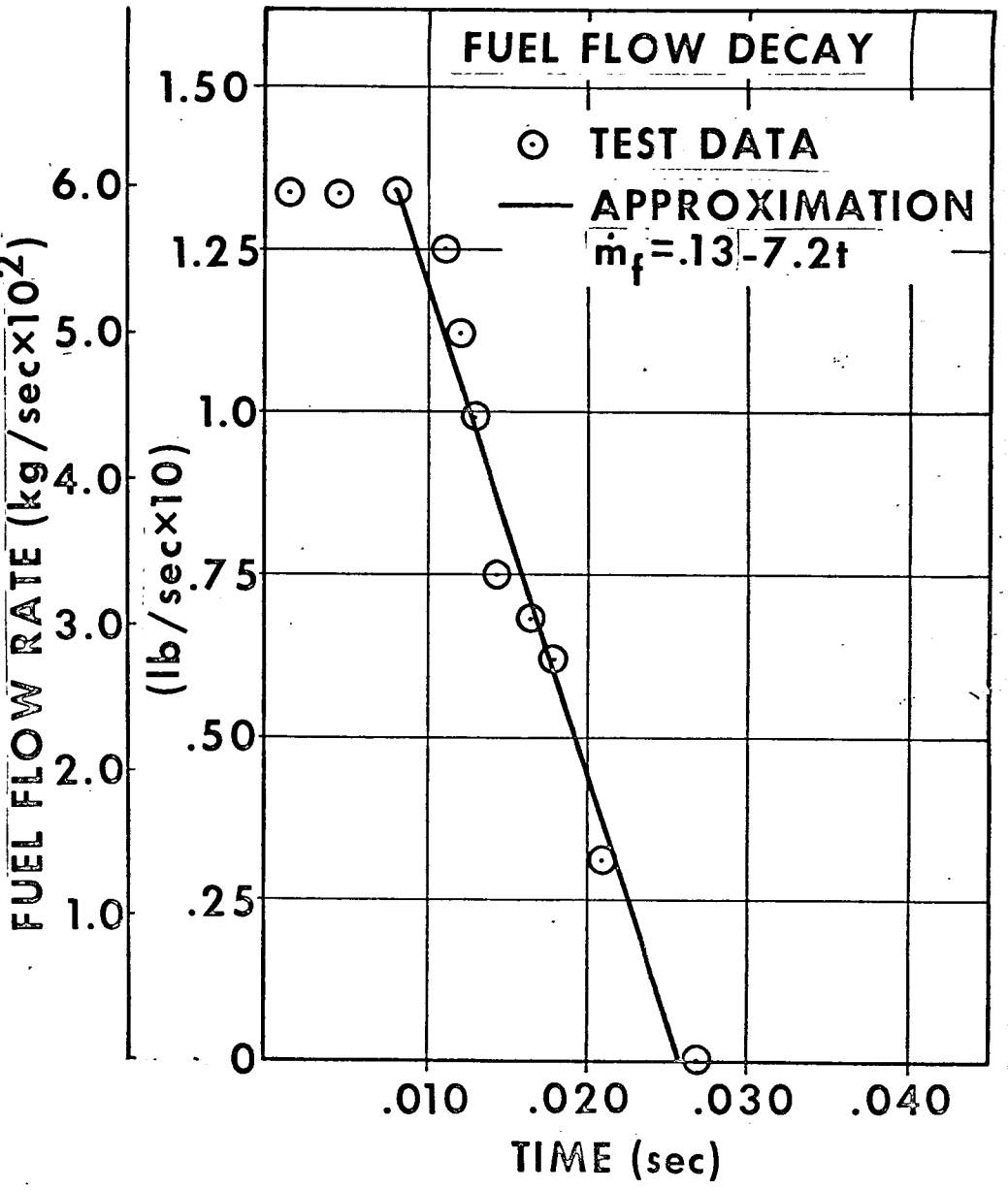
FUEL FLOW DECAY
TEST DATA
APPROXIMATION
$\dot{m}_f$=.13-7.2t
FUEL FLOW RATE (kg/sec×10²)
(lb/sec×10)
TIME (sec)
6.0
5.0
4.0
3.0
2.0
1.0
0
1.50
1.25
1.0
.75
.50
.25
0
.010
.020
.030
.040